Research Article

Experimental investigation and modelling of MQL assisted turning process during machining of 15-5 PH stainless steel using response surface methodology

P. Sivaiah[1]

Abstract

Built-up-edge formation is one of the problems in conventional (flood) machining of 15-5 precipitated hardened stainless steel (PH SS) which results in poor product quality. Further, concentration on stringent environmental conscious regulations has been increasing in metal cutting industries due to environmental pollution. The present work target is to address these problems using minimum quantity lubrication (MQL) machining technique. MQL machining technique is one of the promising techniques for the metal cutting industries because it satisfies the stringent environmental conscious regulations set for metal cutting industries in terms of usage and disposal of chemically contaminated emulsion based coolants. In the present work, studied the effect of MQL cooling, process parameters on turning performance characteristics and also established a relationship between the turning controllable process parameters and responses in the machining of 15-5 PH SS using response surface methodology (RSM) under MQL environment with tungsten carbide cutting insert. Spindle speed (*v*), feed rate (*f*), depth of cut (*d*) and MQL flow rate (*Q*) have been taken as MQL machining process parameters. Output turning performances considered were surface roughness (R_a), tool flank wear (T_w) and material removal rate respectively. Experiments were done based on the central composite design of RSM. From RSM analysis, it was noticed that developed mathematical models predicted the performance results close to the experimental results. Further, it was observed that surface roughness and tool wear reduced significantly with an increase in MQL flow rate respectively.

Keywords Response surface methodology · Minimum quantity lubrication · Machining · Surface roughness · Flank wear · Material removal rate · 15-5 PH SS

1 Introduction

15-5 PH SS contains a maximum of 15% chromium and 5% nickel which give both austenitic and martensite phase characteristics. This steel can be hardened by the aging process which provides high strength, high toughness and sound corrosion resistance. Therefore, this material has been used in many applications in aerospace parts like gears, air fittings, valve parts, impellers and components of nuclear reactors [1]. Any machined product quality substantially depends on the R_a, if it is low then properties such as corrosion resistance, fatigue resistance and thermal resistance enhances. Because of these reasons, nowadays metal cutting industries focus on improving R_a, but machining of 15-5 PH SS develops more adhesion wear and poor surface finish [2]. Hence, usage of cutting fluid is mandatory to reduce the higher cutting temperatures while machining 15-5 PH SS. Cutting fluids provide lubrication effect at the primary and secondary heat generation sources at the cutting zone which leads to an improvement in the machinability of difficult to cut materials by reducing cutting region temperature. Various cooling

✉ P. Sivaiah, sivaiah.337@gmail.com | [1]Department of Mechanical Engineering, Madanapalle Institute of Technology & Science, Madanapalle, Andhra Pradesh 517325, India.

SN Applied Sciences (2019) 1:913 | https://doi.org/10.1007/s42452-019-0827-3

Received: 10 April 2019 / Accepted: 21 June 2019 / Published online: 24 July 2019

techniques have been developed in order to control the cutting region temperature and overall efficiency increments in the machining processes such as flood cooling, air/gas/vapour, MQL, cryogenic cooling and high pressure cooling [3]. Among all, the most prominent system is the use of flood cooling but an issue with flood cooling is that it takes time to cool the real cutting area due to the failure of infiltration of coolant between the chip-tool interface causes reduction in tool life and poor surface finish [4]. One more issue with flood cooling is that it damages the environment and health of an operator in the metal cutting industry [5]. Attempts have been done for environmental protection by replacing the flood cooling technique with MQL cooling technique. In MQL, small quantity lubricant is atomized by a certain high pressure gas and jetted to the machining area, cooling effects are mainly achieved by the high pressure gas [6]. MQL is a green machining technology and use of this reduces the cost of cutting fluid consumption. Environmental pollution and handling cost can be further reduced by using vegetable oil as cutting fluid [7]. Khan and Dhar [8] investigated about vegetable oils that this can be used in the same operations as mineral based, or petroleum-based, fluids. Sharma and Sidhu [7] used vegetable oil as coolant while turning of AISI D2 steel under MQL cooling environment. They found a substantial improvement in the turning process performance characteristics in MQL condition due to the significant reduction of machining zone temperature when compared dry machining condition. Sivaiah and Chakradhar [9–11] performed turning experiments on 17-4 PH SS under MQL, wet and dry machining environments. They found a significant reduction in R_a, T_w under MQL environment over the wet and dry machining environments. They claimed that beneficial results in MQL are due to the substantial control of adhesion wear on the cutting tool.

For developing a mathematical model, it is very much necessary to perform experiments and get the response data which is a function of spindle speed, feed rate, depth of cut and MQL flow rate. Nowadays design of experiments (DOE) is a quite extensively used in machinability studies. Statistical DOE is the process of planning experiments in order to analyze the appropriate data by statistical methods which give an objective and valid conclusion. Nevertheless, widely used DOE are full factorial design, Taguchi, RSM and one factor at a time approach [12]. Thiele and Melkote [13] performed finish hard turning operation on AISI H13 steel by using 4-factor and 2-level fractional factorial design. Arbizu and Perez [14] developed the prediction model for surface roughness by using RSM for determining the surface quality in the turning process. Choudhury and Baradie [15] performed turning of high strength tool and used 2- factor and 3- level factorial design to estimate the R_a using RSM. Sarikaya and Gullu [16] performed experiments on turning of AISI 1050 steel using RSM design by considering process parameters namely *v, f, d* and *Q* respectively and studied the different surface quality characteristics. From the results, they claimed that MQL is one of the best machining technique to improve product quality. In another work, they found a better result in terms of T_w and R_a in MQL cooling condition while machining Haynes 25 super alloy compared to dry and wet machining respectively [17]. Gupta et al. [18] considered *v, f* and side cutting edge angle as controllable process parameters for investigating the different turning performance characteristics while machining of titanium alloy (Grade-II) using RSM under the MQL environment. From confirmation test results, they found that RSM developed mathematical equations predicted the turning performance characteristics very close to the experimental results within the given range. Few researchers worked on 15-5 PH SS in metal removing processes as follows. Palanisamy and Senthil [19] worked on turning of laser surface treated 15-5 PH SS under the dry environment and found beneficial performance results when compared to without treated 15-5 PH SS material. Similarly, Junior and Diniz have studied the machinability indexes in milling process while machining of 15-5 PH SS material [2]. Yıldırım et al. [20] performed milling experiments on Waspaloy by considering cutting oil type, fluid flow rate, milling method, spray distance and nozzle type as process parameters whereas tool life and cutting forces are taken as responses. In a while, modelling and optimization studies have been carried out and validated through confirmation tests respectively. Gupta et al. [21] observed improved turning performance with Ranque–Hilsch vortex tube nitrogen minimum quantity lubrication when compared to dry cutting, nitrogen cooling and nitrogen minimum quantity lubrication respectively during turning of Al 7075-T6 alloy. Sarikaya and Gullu [22] applied Taguchi based Gray relational analysis and determined the optimum cutting conditions in terms of the type of coolant and MQL coolant flow rate and cutting velocity while turning of Haynes 25 superalloy. Further, the effect of these variables on tool wear and surface roughness has been studied using 3D surface plots. Sivaiah and Chakradhar [23] conducted experiments based on the L20 RSM based CCD design and developed mathematical models for surface roughness, tool wear and MRR while turning of 17-4 PH SS material under cryogenic cooling condition. Conformation experimental results showed good agreement with predicted results. In the literature, few studies have been carried out to select the optimum process parameters and cooling type during turning of PH SS grade material under different sustainable machining techniques [24–30]. Sampaio et al. [31] performed comparative studies in turning of SAE1045 steel under dry and MQL cutting condition respectively. From the study, it was found that abrasive wear as prominent wear mechanism under both cutting conditions. Further, observed a significant reduction in cutting force, tool wear and white layer depth in MQL over dry cutting respectively. Tamang et al. [32] beneficial results were observed with MQL cutting condition due to good lubrication effect over dry condition while turning of Inconel 825 material. Subsequently, optimum process parameters were determined using a genetic algorithm to solve multi objective problem.

It is clear from the literature study that statistical technique such as RSM is very much effective for cost-effective research to model any manufacturing process. 15-5 PH SS has many industrial applications; hence, an extensive experimental study was carried out on it. In this study, vegetable oil has been taken as MQL coolant to completely overcome the problems which come from harmful mineral and petroleum-based coolants. From the literature study, it was found that no attempt was done on mathematical model development and analyzes of machining parameters and responses while turning of 15-5 PH SS with tungsten carbide (WC) tool under the MQL cooling environment using RSM. Development of predictive mathematical models in turning of 15-5 PH SS under MQL cooling conditions will helpful for cost-effective research in metal cutting industries. Hence, in the present work, this attempt is fulfilled. In this reported work, machining parameters such as spindle speed, feed rate, depth of cut, and MQL flow rate were considered as independent variables and effect of these machining parameters on R_a, MRR and T_w have been investigated further using RSM analysis.

2 Materials and methods

KIRLOSKAR lathe has been used to perform the turning experiments on 15-5 PH SS round bars with 30 mm diameter and 150 mm length under MQL cooling environments. The chemical composition of the workpiece is as follows: Fe-75%, Cr-14.48%, Ni-4.5%, Cu-3.5%, Mn ≤ 1%, Si ≤ 1%, Nb + Ta-0.3%, C ≤ 0.07%, P ≤ 0.04%, S ≤ 0.03%. Uncoated tungsten carbide (SNMG 120408MP) KC5010 of Kennametal made were fixed in a tool holder of PSBNR 2020K12. The controllable process parameters and their levels considered for the present study are shown in Table 1. Working insert tool geometry is as follows: inclination angle: − 6°, rake angle: − 6°, clearance angle: 6°, Nose radius: 0.8 mm, major cutting edge angle: 75. Pilot experiments were performed for fixing the ranges for each controllable process parameter. To reduce the test quantities and to maximize the quality of results, RSM experimental design is one of the efficient designs [12]. For experimental investigation and developing the predictive models for responses under the MQL environment, 30 experiments were conducted according to the RSM based CCD and results were shown in Table 2. CCD is the best suited for second order model to obtain the entire area of interest in the cubic space [12]. In the present work, RSM analysis was carried out in Design Expert 10.0 Software. Second order polynomial regression model called quadratic model has been used to predict the response models for R_a, T_w and MRR respectively under the MQL environment. DROPCO made MQL setup has been used in the present study and MQL mist supply at the machining zone is shown Fig. 1. Emulsion-based coolant is mixed in the water in the ratio of 1:20 and mixed is used as a MQL coolant. MQL is supplied with a compressed air pressure of 4 bars to obtain the mist.

2.1 Equipments used and it measurement procedure for output responses

Mitutoyo surftest, SJ-301 model was used to measure the R_a of the machined surfaces. Five R_a measurements were taken on each machined sample and average was taken as actual R_a value. Zeiss make optical microscope has been used for measuring tool flank wear. Constant machining time considered for the tool wear investigation is 4 min. The MRR values were calculated by using the Eq. (1), 4 min machining time was considered to calculate MRR. Workpiece material weight before and after machining was measured with the help of 'Contech' made 'CA 3102' model digital weighing scale with a maximum weight capacity of 3.2 kg and accuracy of 0.01 g.

$$\mathrm{MRR}\ (\mathrm{g/min}) = \left(W_b - W_f\right)/t \quad (1)$$

Table 1 Machining parameters and their levels

Parameters	Units	Low level (− 1)	Medium level (0)	High level (+ 1)
Cutting speed (A)	rpm	315	545	775
Feed rate (B)	mm/rev	0.048	0.0955	0.143
Depth of cut (C)	mm	0.2	0.4	0.6
MQL flow rate (D)	ml/h	50	75	100

Table 2 RSM L_{30} design matrix layout and experimental results

S. no	Machining parameters				Responses		
	Cutting speed (rpm)	Feed rate (mm/rev)	Depth of cut (mm)	MQL flow rate (ml/h)	Ra (μm)	MRR (g/min)	Tw (mm)
1	315	0.048	0.2	50	0.7	4.63	0.73
2	775	0.048	0.2	50	0.24	7.38	0.78
3	315	0.143	0.2	50	1.19	5.79	0.81
4	775	0.143	0.2	50	0.78	8.11	0.82
5	315	0.048	0.6	50	1.39	15.7	1.26
6	775	0.048	0.6	50	1.02	16.81	1.32
7	315	0.143	0.6	50	1.72	16.1	1.29
8	775	0.143	0.6	50	1.25	18.71	1.4
9	315	0.048	0.2	100	0.63	8.87	0.66
10	775	0.048	0.2	100	0.18	9.08	0.74
11	315	0.143	0.2	100	1.11	8.92	0.78
12	775	0.143	0.2	100	0.6	9.38	0.79
13	315	0.048	0.6	100	1.3	16.1	1.21
14	775	0.048	0.6	100	0.97	17.2	1.3
15	315	0.143	0.6	100	1.66	16.5	1.26
16	775	0.143	0.6	100	1.14	19.2	1.37
17	315	0.0955	0.4	75	1.31	10.69	0.81
18	775	0.0955	0.4	75	0.99	13.19	0.95
19	545	0.048	0.4	75	1.13	11.21	0.85
20	545	0.143	0.4	75	1.2	13.29	0.98
21	545	0.0955	0.2	75	0.65	4.63	0.73
22	545	0.0955	0.6	75	1.23	17.01	1.3
23	545	0.0955	0.4	50	1.21	11.21	0.85
24	545	0.0955	0.4	100	1.09	13.29	0.98
25	545	0.0955	0.4	75	1.21	11.19	0.82
26	545	0.0955	0.4	75	1.1	11.99	0.9
27	545	0.0955	0.4	75	1.13	13.15	0.92
28	545	0.0955	0.4	75	1.11	13.26	0.97
29	545	0.0955	0.4	75	1.12	11.88	0.87
30	545	0.0955	0.4	75	1.13	13.2	0.96

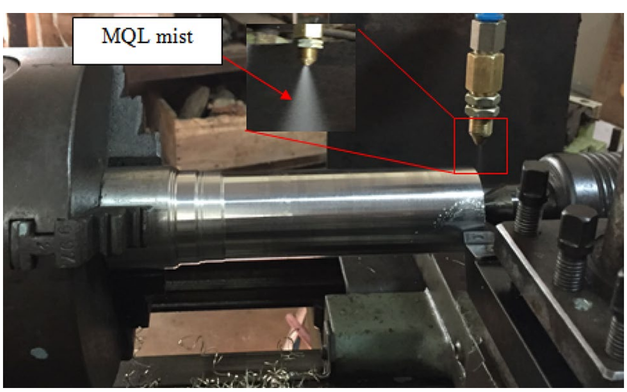

Fig. 1 MQL machining zone

where W_b Workpiece weight before machining (g); W_f Workpiece weight after 4 min machining (g); t Machining time (min).

3 Result and discussion

Quadratic models for R_a, T_w and MRR were established by using the Design Expert software. For the developed model, adequacy and significant tests have been performed for each response. The model adequacy checks include significant on the model coefficient test, significant of the regression mode test, lack of fit test, coefficients of determinations (R^2) and examination of residuals [33]. ANOVA results of each response have been used to analyze the adequacy tests.

Table 3 ANOVA table for R_a (before elimination)

Source	Sum of squares	DOF	Mean square	F-value	*p* value Prob. > F
Model	3.37	14	0.24	54.57	< 0.0001 (significant)
A	0.82	1	0.82	185.83	< 0.0001
B	0.53	1	0.53	120.33	< 0.0001
C	1.74	1	1.74	395.21	< 0.0001
D	0.037	1	0.037	8.47	0.0108
AB	5.625E−003	1	5.625E−003	1.28	0.2764
AC	1.225E−003	1	1.225E−003	0.28	0.6058
AD	6.250E−004	1	6.250E−004	0.14	0.7118
BC	0.044	1	0.044	10.00	0.0064
BD	1.600E−003	1	1.600E−003	0.36	0.5559
CD	4.000E−004	1	4.000E−004	0.091	0.7674
A^2	4.486E−004	1	4.486E−004	0.10	0.7541
B^2	2.054E−003	1	2.054E−003	0.47	0.5052
C^2	0.10	1	0.10	22.77	0.0002
D^2	4.486E−004	1	4.486E−004	0.10	0.7541
Residual	0.066	15	4.408E−003		
Lack of fit	0.058	10	5.839E−003	3.78	0.0778 (not significant)
Pure error	7.733E−003	5	1.547E−003		
Cor. total	3.43	29			
Standard deviation = 0.066			R-squared = 0.9807		
Mean = 1.05			Adj R-squared = 0.9628		
Coefficient of variation % = 6.33			Pred R-squared = 0.9135		
Predicated residual error of sum of squares (PRESS) = 0.30			Adeq. precision = 31.595		

Table 4 ANOVA table for R_a (after backward elimination)

Source	Sum of squares	DOF	Mean square	F-value	*p* value Prob. > F
Model	3.35	6	0.56	156.38	< 0.0001 (significant)
A	0.82	1	0.82	229.32	< 0.0001
B	0.53	1	0.53	148.49	< 0.0001
C	1.74	1	1.74	487.70	< 0.0001
D	0.037	1	0.037	10.46	0.0037
BC	0.044	1	0.044	12.34	0.0019
C^2	0.18	1	0.18	50.00	< 0.0001
Residual	0.082	23	3.572E−003		
Lack of fit	0.074	18	4.135E−003	2.67	0.1402 (not significant)
Pure error	7.733E−003	5	1.547E−003		
Cor. total	3.43	29			
Standard deviation = 0.060			R-squared = 0.9761		
Mean = 1.05			Adj R-squared = 0.9698		
Coefficient of variation % = 5.69			Pred R-squared = 0.9616		
Predicated residual error of sum of squares (PRESS) = 0.13			Adeq. precision = 51.378		

3.1 Analysis of surface roughness

Tables 3 and 4 respectively show the before and after backward elimination of ANOVA tables for a quadratic model for R_a. The *p* value for the model is lower than 0.05 (i.e. α = 0.05 or 95% confidence) therefore model is statistically significant. Desired 'lack of fit' should be nonsignificant. From Table 3, the model is statistically significant and 'lack of fit' is nonsignificant. From Table 3, factor A, factor B, factor C, factor D, the interaction effect of factor B with factor C and second order term of factor C are identified as the significant terms at 95% confidence interval. To fit the quadratic model for R_a, in Table 3, appropriate non-significant terms ($p > 0.05$) were eliminated by backward elimination process and the ANOVA results for the reduced model were represented in Table 4. Now the reduced model is significant ($p < 0.05$) and 'lack of fit' is nonsignificant. In Table 4, the value of R^2 and adjusted R^2 97.61% and 96.98% respectively are very close to each other which mean the regression model explained a close relationship between the factors (independent) and response R_a. When R^2 approaches unity, the response model fits the actual data because of the difference between the predicted and actual values of response become small. Figure 2 shows that errors are normally distributed because of errors are structured around a straight line. Adeq-precision measures the signal-to-noise ratio. A ratio greater than 4 is desirable means higher signal. Equations (2) and (3) indicate the reduced final predicted R_a in terms of actual and coded factors respectively.

In coded terms

$$R_a = 1.14 - 0.21 * A + 0.17 * B + 0.31 * C - 0.046 * D - 0.053 * B * C - 0.16 * C^2 \quad (2)$$

In actual factors

$$R_a = -0.022 - 9.275 * 10^{-4} * v + 5.824 * f + 5.233 * d - 1.822 * 10^{-3} * Q - 5.526 * f * d - 3.937 * d^2 \quad (3)$$

The estimated response surface for R_a in relation to the design parameters of 'f' and 'd' is shown in Fig. 3. It seen from Fig. 3 that R_a increases with increase in the 'f' and 'd' respectively. This is due to the more tool wear at the higher 'f' and 'd' cutting conditions (Refer Fig. 12). Figure 3 shows the combination of lowers value of f (0.048 mm/rev) and d (0.2 mm) generates low R_a value.

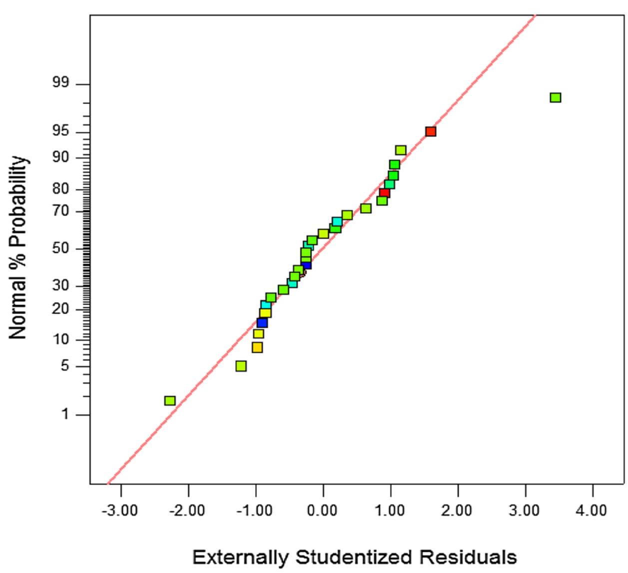

Fig. 2 Normal probability plot of the residuals for R_a

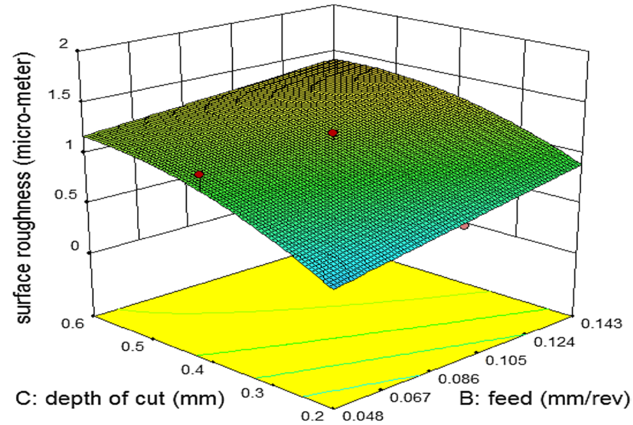

Fig. 3 Response surface plot of R_a according to change of feed rate and depth of cut

The interaction effect of 'd' and 'Q' on estimated response surface for R_a is shown in Fig. 4. From Fig. 4, it was perceived that R_a increases with a rise in 'd' whereas it decreases with the rise in 'Q'. This is because as the 'Q' increase the friction at the cutting zone reduces, causes low T_w resulting in few tool marks and control of material side flow from the tool. Figure 5 shows the SEM images obtained at the given condition. It is clear from Fig. 4 that the best surface finish is obtainable at the low levels of 'd' (0.2 mm) and at a high level of 'Q' (100 ml/h). So, a higher level of 'Q' should be used for better obtaining low R_a. In the literature, observed Sarikaya and Gullu [16] similar findings while turning of AISI 1050 material using RSM.

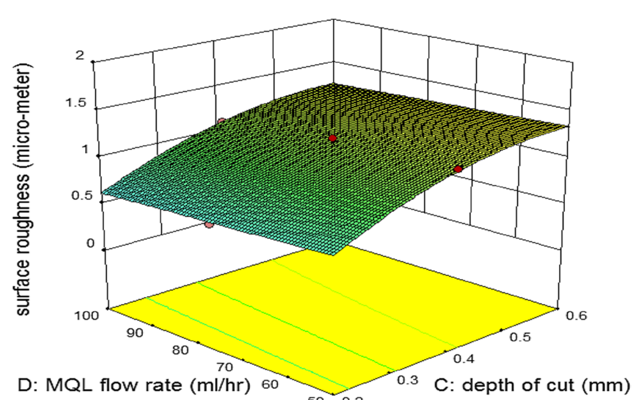

Fig. 4 Response surface plot of R_a according to change of depth of cut and MQL flow rate

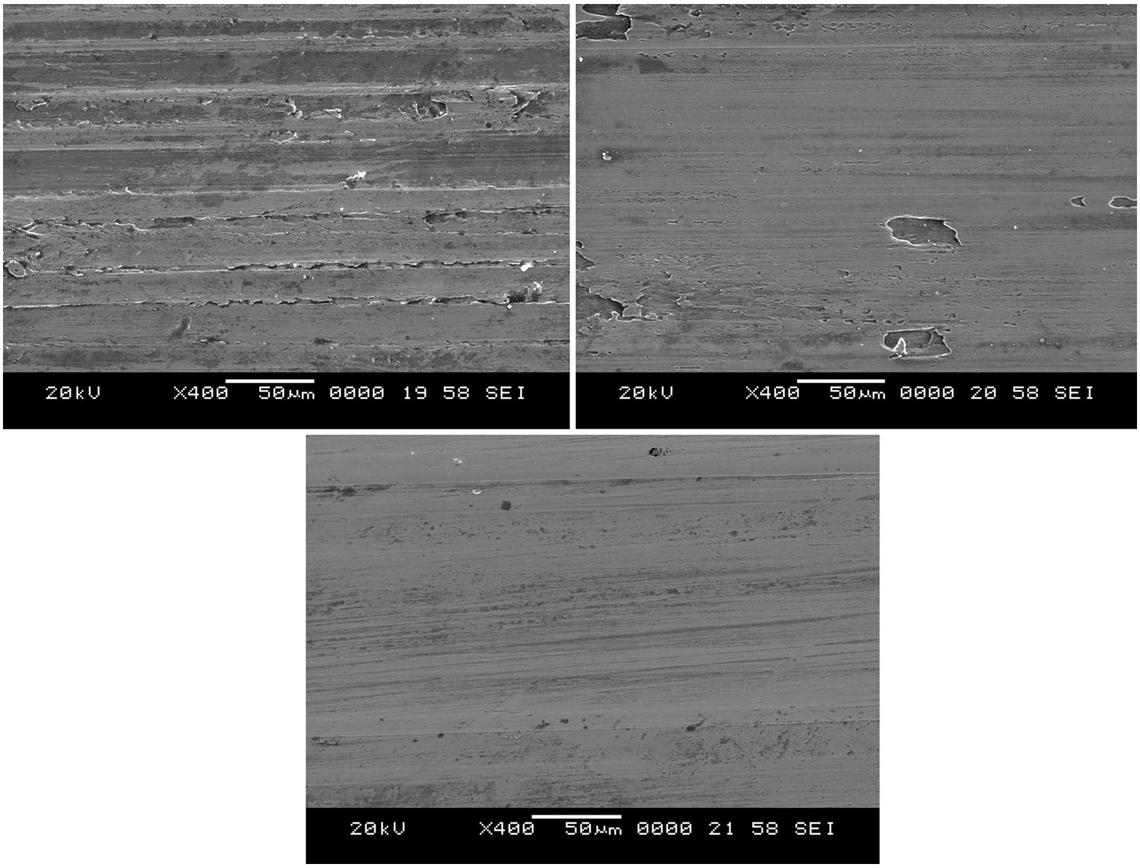

Fig. 5 SEM images of machined surfaces at **a** $v=315$ rpm, $f=0.048$ mm/rev, $d=0.2$ mm and $Q=50$ ml/h, **b** $v=545$ rpm, $f=0.096$ mm/rev, $d=0.4$ mm and $Q=75$ ml/h, **c** $v=775$ rpm, $f=0.096$ mm/rev, $d=0.4$ mm and $Q=75$ ml/h

3.2 Analysis of material removal rate

Table 5 represents the ANOVA results for MRR. From Table 5, the quadratic model is significant and 'lack of fit' is nonsignificant which are desired. However, few model terms are insignificant ($p>0.05$) and those terms were eliminated by back elimination method. From Table 5, Factor A (v), factor B (f), factor C (d), factor D (Q) and interaction effect of factor C (d) with factor D (d) were recognized as significant terms. Table 6 shows the ANOVA results for the reduced model. From Table 6, it was found that the model is still significant and 'lack of fit' is nonsignificant. The respective value of R^2 and adjusted R^2 are 96.01% and 95.18% comparatively close. Adeq-Precision is greater than 4. Figure 6 shows that the residuals are falling on a straight line, which means that the errors are normally distributed. The final estimated regression model for MRR is indicated in Eqs. (4) and (5) in the coded and actual factors respectively.

In coded terms

$$\begin{aligned} \text{MRR} = {} & 12.26 + 0.88 * \text{A} + 0.50 * \text{B} \\ & + 4.81 * \text{C} + 0.78 * \text{D} - 0.54 * \text{C} * \text{D} \end{aligned} \tag{4}$$

In actual factors

$$\begin{aligned} \text{MRR} = {} & -6.039 + 3.806 * 10^{-3} * v + 10.549 * f \\ & + 32.15764 * d + 0.074 * Q - 0.108 * d * Q \end{aligned} \tag{5}$$

The interaction effect of 'f' and 'd' on MRR is shown in Fig. 7. Figure 7 shows that MRR increases with an increase in 'f' and 'd' respectively. This effect is due to the rise in the rate of plastic deformation at the higher cutting conditions. It is clear from Fig. 7 that the higher MRR is obtainable at the high 'f' (0.143 mm/rev) and high 'd' (0.6 mm). Figure 8 shows the interaction effect of 'd' and 'Q' on MRR. From Fig. 8, it is noticed that as 'd' and 'Q' increases then MRR also increases. This is because of less tool wear obtained at the high flow rates. It was also observed from Fig. 8 that at maximum levels of 'd' (0.6 mm) and 'Q'(100 ml/h) could cause for higher MRR.

3.3 Analysis of tool flank wear

Table 7 represents the ANOVA results for T_w before elimination of nonsignificant terms. The model terms like A, B,

Table 5 ANOVA table for MRR (before elimination)

Source	Sum of squares	DOF	Mean square	F-value	*p* value Prob. > F
Model	455.69	14	32.55	37.19	< 0.0001 (significant)
A	13.80	1	13.80	15.77	0.0012
B	4.52	1	4.52	5.16	0.0382
C	416.07	1	416.07	475.37	< 0.0001
D	11.05	1	11.05	12.62	0.0029
AB	0.53	1	0.53	0.61	0.4474
AC	0.20	1	0.20	0.23	0.6412
AD	1.17	1	1.17	1.33	0.2664
BC	0.38	1	0.38	0.43	0.5209
BD	0.13	1	0.13	0.15	0.7058
CD	4.69	1	4.69	5.36	0.0352
A^2	0.095	1	0.095	0.11	0.7468
B^2	0.65	1	0.65	0.74	0.4021
C^2	2.24	1	2.24	2.55	0.1309
D^2	0.65	1	0.65	0.74	0.4021
Residual	13.13	15	0.88		
Lack of fit	9.30	10	0.93	1.21	0.4403 (not significant)
Pure error	3.83	5	0.77		
Cor. total	468.82	29			
Standard deviation = 0.94			R-squared = 0.9720		
Mean = 12.26			Adj R-squared = 0.9459		
Coefficient of variation % = 7.63			Pred R-squared = 0.8905		
Predicated residual error of sum of squares (PRESS) = 51.33			Adeq. precision = 21.422		

Table 6 ANOVA table for MRR (after backward elimination)

Source	Sum of squares	DOF	Mean square	F-value	*p* value Prob. > F
Model	450.12	5	90.02	115.53	< 0.0001 (significant)
A	13.80	1	13.80	17.71	0.0003
B	4.52	1	4.52	5.80	0.0241
C	416.07	1	416.07	533.96	< 0.0001
D	11.05	1	11.05	14.17	0.0010
CD	4.69	1	4.69	6.02	0.0218
Residual	18.70	24	0.78		
Lack of fit	14.87	19	0.78	1.02	0.5445 (not significant)
Pure error	3.83	5	0.77		
Cor. total	468.82	29			
Standard deviation = 0.88			R-squared = 0.9601		
Mean = 12.26			Adj R-squared = 0.9518		
Coefficient of variation % = 7.20			Pred R-squared = 0.9420		
Predicated residual error of sum of squares (PRESS) = 27.20			Adeq. precision = 35.301		

C and C^2 are significant. To fit the quadratic model for T_w appropriate, the nonsignificant terms are eliminated by a backward elimination process. The ANOVA results of the reduced quadratic model for T_w are shown in Table 8. The reduced model results indicate that the model is significant ($p < 0.05$) and 'lack of fit' is nonsignificant ($p > 0.05$). The R^2 and adjusted R^2 values 97.15% and 96.70% respectively are close to each other. By seeing Fig. 9, it was observed that errors are normally distributed due to residuals are falling on a straight line. Equations (6) and (7) indicates the final predictive models for T_w in terms of coded and actual factors.

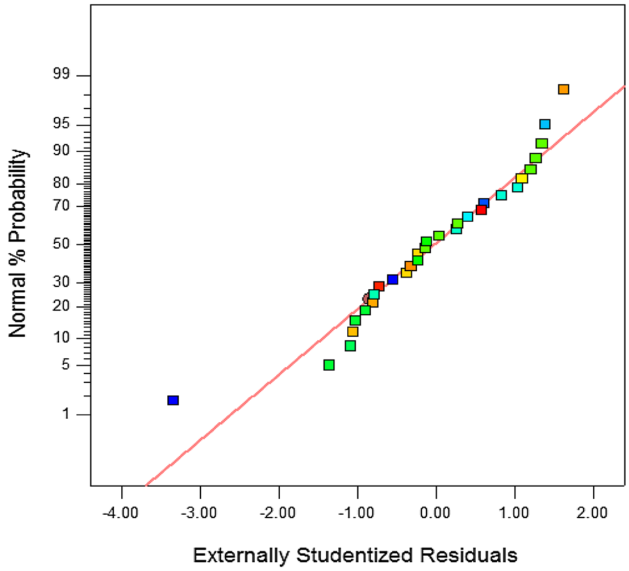

Fig. 6 Normal probability plot of the residuals for MRR

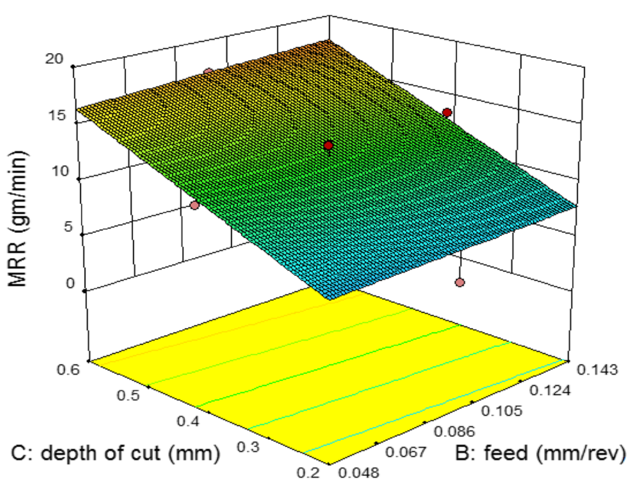

Fig. 7 Response surface plot of MRR according to change of feed rate and depth of cut

In coded terms

$$T_w = 0.91 + 0.037 * A + 0.036 * B + 0.27 * C + 0.13 * C^2 \quad (6)$$

In actual factors

$$\begin{aligned} T_w = {} & 0.706 + 1.594 * 10^{-4} * v \\ & + 0.760 * f - 1.158 * d + 3.138 * d^2 \end{aligned} \quad (7)$$

The influence of interaction in terms of 'f' and 'd' on T_w is shown in Fig. 10. Figure 10 reveals that the T_w increases with an increase in the '*f*' and '*d*' values. This result in rise of machining zone temperatures at the higher values of

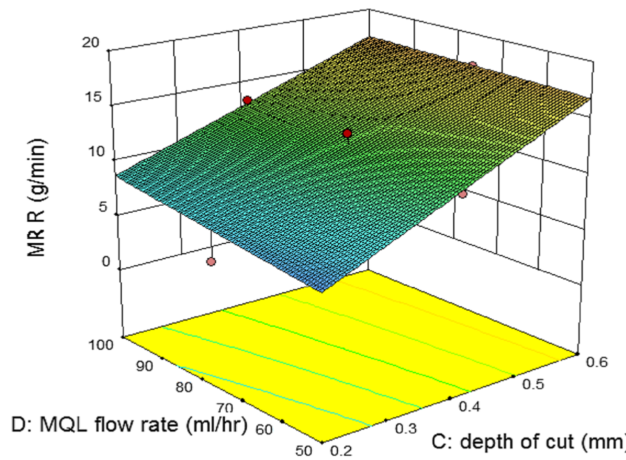

Fig. 8 Response surface plot of MRR according to change of depth of cut and MQL flow rate

'*f*' and '*d*' respectively. From Fig. 10, it can be predicted that lower levels of '*f*' (0.048 mm/rev) and '*d*' (0.2 mm) produced low T_w.

Figure 11 shows the effect of interaction factors of '*d*' and '*Q*' on T_w. It was observed that T_w increases with increase in '*d*' and decreases with an increase in '*Q*' as depicted in Fig. 11. From Fig. 11, As the '*Q*' increases then friction at the contacting asperities reduces resulting in low machining zone temperature leads to low T_w. It was also noticed that at the low level of '*d*' (0.2 mm) and a high level of '*Q*' (100 ml/h) could produce low T_w. Figure 12 shows the SEM images of T_w at different cutting conditions. From Fig. 12, abrasion wear is found as leading wear mechanism due to the tool-workpiece contact nature and cutting forces. These findings match with the results in the literature [18].

4 Conformation experiment

To validate the RSM predicted models, three confirmation experiments were performed for the R_a, MRR and tool wear. To carry out the confirmation test, process parameters values were selected within the assumption range in the study. The predicted values were obtained through developed predictive models and actual values were obtained by performing the experiments at selected levels. Both predicted and actual results were compared and the percentage errors were calculated. Confirmation test results are listed in Table 9. It is observed that the percentage errors are very small between the predicted and experimental values for all the responses in the study. In the literature, similar results were found [34, 35].

Table 7 ANOVA table for T_w (before elimination)

Source	Sum of squares	DOF	Mean square	F-value	*p* value Prob. > F
Model	1.49	14	0.11	44.47	< 0.0001 (significant)
A	0.024	1	0.024	10.14	0.0062
B	0.023	1	0.023	9.83	0.0068
C	1.32	1	1.32	551.88	< 0.0001
D	1.606E−003	1	1.606E−003	0.67	0.4250
AB	1.000E−004	1	1.000E−004	0.042	0.8406
AC	3.025E−003	1	3.025E−003	1.27	0.2780
AD	2.250E−004	1	2.250E−004	0.094	0.7631
BC	2.250E−004	1	2.250E−004	0.094	0.7631
BD	2.250E−004	1	2.250E−004	0.094	0.7631
CD	1.000E−004	1	1.000E−004	0.042	0.8406
A^2	9.301E−004	1	9.301E−004	0.39	0.5419
B^2	6.676E−004	1	6.676E−004	0.28	0.6047
C^2	0.035	1	0.035	14.62	0.0017
D^2	6.676E−004	1	6.676E−004	0.28	0.6047
Residual	0.036	15	2.387E−003		
Lack of fit	0.020	10	1.988E−003	0.62	0.7546 (not significant)
Pure error	0.016	5	3.187E−003		
Cor. total	1.52	29			
Standard deviation = 0.049			R-squared = 0.9765		
Mean = 0.98			Adj R-squared = 0.9545		
Coefficient of variation % = 4.98			Pred R-squared = 0.9245		
Predicated residual error of sum of squares (PRESS) = 0.11			Adeq. precision = 20.453		

Table 8 ANOVA table for T_w (after backward elimination)

Source	Sum of squares	DOF	Mean square	F-value	*p* value Prob. > F
Model	1.48	4	0.37	213.37	< 0.0001 (significant)
A	0.024	1	0.024	13.97	0.0010
B	0.023	1	0.023	13.55	0.0011
C	1.32	1	1.32	760.45	< 0.0001
C^2	0.11	1	0.11	65.51	< 0.0001
Residual	0.043	25	1.733E−003		
Lack of fit	0.027	20	1.369E−003	0.43	0.9194 (Not significant)
Pure error	0.016	5	3.187E−003		
Cor. total	1.52	29			
Standard deviation = 0.042			R-squared = 0.9715		
Mean = 0.98			Adj R-squared = 0.9670		
Coefficient of variation % = 4.25			Pred R-squared = 0.9617		
Predicated residual error of sum of squares (PRESS) = 0.058			Adeq. precision = 40.408		

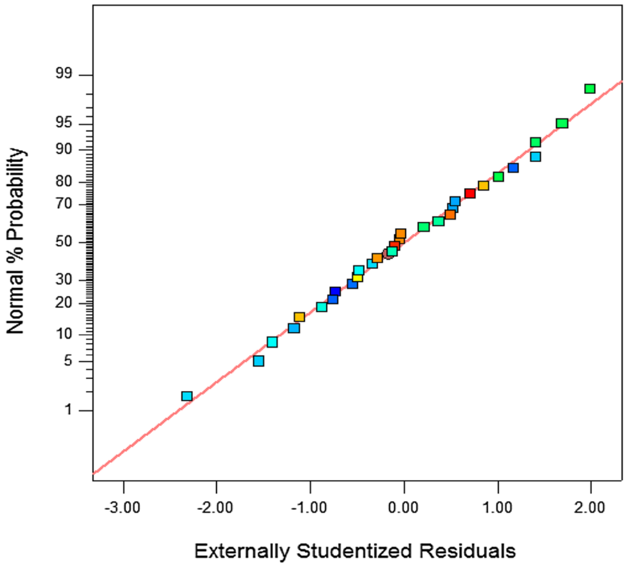

Fig. 9 Normal probability plot of the residuals for T_w

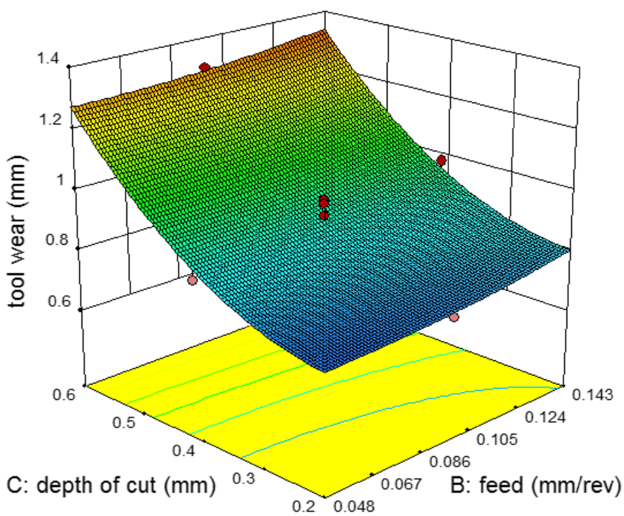

Fig. 10 Response surface plot of T_w according to change of feed rate and depth of cut

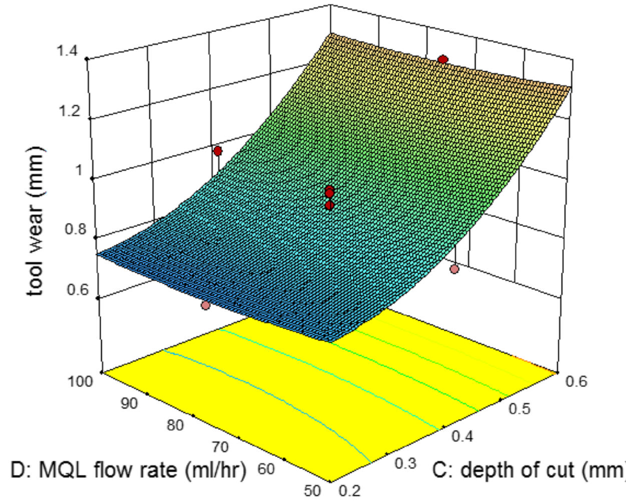

Fig. 11 Response surface plot of T_w according to change of depth of cut and MQL flow rate

5 Conclusions

- In MQL machining, the surface roughness increases with an increase in the feed rate and depth of cut whereas decreases with an increase in MQL flow rate. The MRR increases with an increase in spindle speed, feed rate, depth of cut and MQL flow rate respectively. The tool flanks wear increases with an increase in the feed rate and depth of cut whereas decreases with increase in MQL flow rate respectively.
- ANOVA revealed that depth of cut is the most influential parameter on surface roughness, flank wear and MRR respectively. Spindle speed and feed rate also have a prominent effect on surface roughness.
- RSM developed models predicted the surface roughness, flank wear and MRR values very close to the experimental results within the specified range in the work.
- It is recommended that while concerning environmental issues, the use of MQL with vegetable oil is much better than flood cooling because there is no problem of disposal of coolant and no recycling cost of coolants.

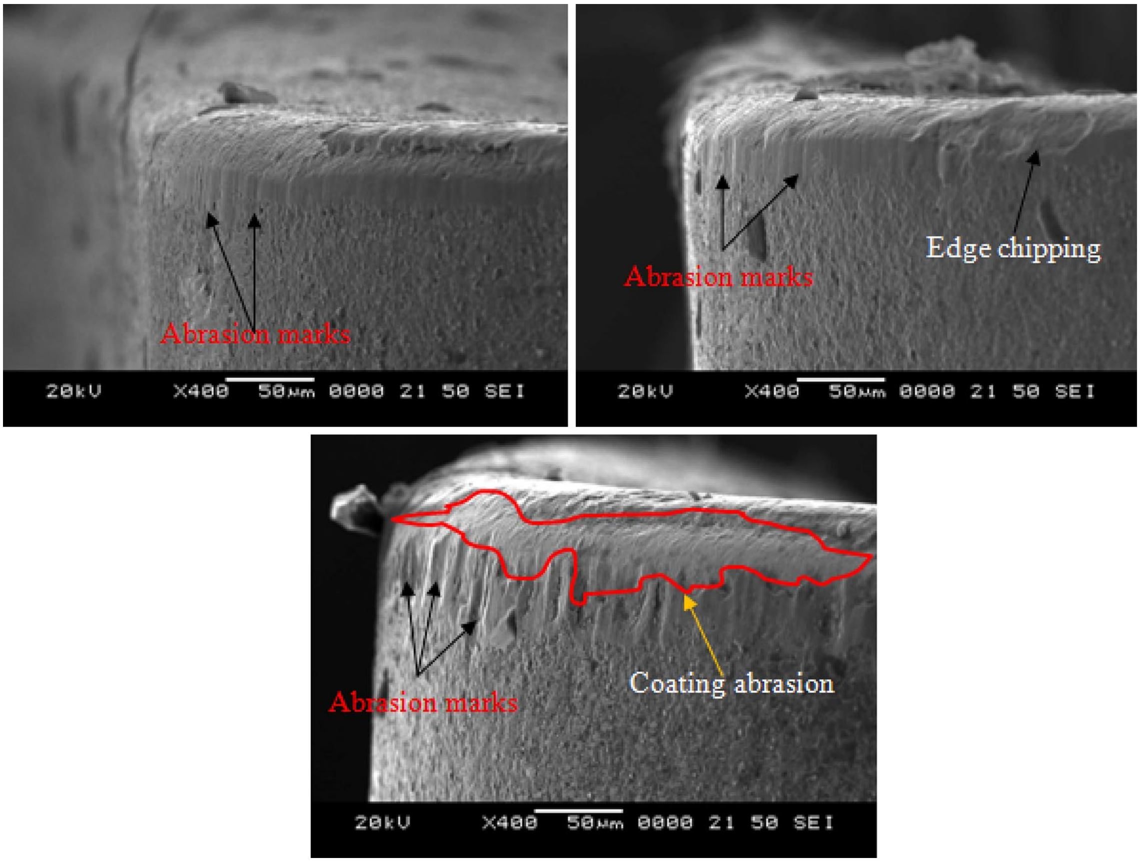

Fig. 12 SEM images of machined surfaces at **a** $v=315$ rpm, $f=0.048$ mm/rev, $d=0.2$ mm and $Q=50$ ml/h, **b** $v=545$ rpm, $f=0.096$ mm/rev, $d=0.4$ mm and $Q=75$ ml/h, **c** $v=775$ rpm, $f=0.096$ mm/rev, $d=0.4$ mm and $Q=75$ ml/h

Table 9 The results of the confirmation test for R_a, MRR and T_w

S. no.	Machining parameters				Surface roughness (µm)			MRR (g/min)			Tool wear (mm)		
	A	B	C	D	Actual	Predicted	Error (%)	Actual	Predicted	Error (%)	Actual	Predicted	Error (%)
1	315	0.048	0.2	50	0.7	0.71	−1.43	4.63	4.74	−2.37	0.73	0.69	5.47
2	545	0.0955	0.4	75	1.21	1.14	5.78	11.19	12.25	−9.47	0.82	0.91	10.97
3	775	0.143	0.6	100	1.14	1.16	−1.75	19.2	18.67	2.76	1.37	1.38	−0.73

Funding This research did not receive any specific grant from funding agencies in the public, commercial, or not-for-profit sectors.

Compliance with ethical standards

Conflict of interest The authors declare that they have no conflict of interest.

References

1. Hsiao CN, Chiou CS, Yang JR (2002) Aging reactions in a 17-4 PH stainless steel. Mater Chem Phys 74(2):134–142
2. Junior AB, Diniz AE, Teixeira Filho F (2009) Tool wear and tool life in end milling of 15-5 PH stainless steel under different cooling and lubrication conditions. Int J Adv Manuf Technol 43(7–8):756–764
3. Sharma VS, Dogra M, Suri NM (2009) Cooling techniques for improved productivity in turning. Int J Mach Tools Manuf 49(6):435–453
4. Shaw MC, Pigott JD, Richardson LP (1951) Effect of cutting fluid upon chip–tool interface temperature. Trans ASME 71(2):45–56
5. Hong SY, Broomer M (2000) Economical and ecological cryogenic machining of AISI 304 austenitic stainless steel. Clean Prod Process 2(3):157–166
6. Endapally KR (2008) Experimental Evaluation of the effect of minimum quantity lubrication in turning AISI-4140 Steel. Doctoral dissertation, University of North Dakota

7. Sharma J, Sidhu BS (2014) Investigation of effects of dry and near dry machining on AISI D2 steel using vegetable oil. J Clean Prod 66:619–623
8. Khan MMA, Dhar NR (2006) Performance evaluation of minimum quantity lubrication by vegetable oil in terms of cutting force, cutting zone temperature, tool wear, job dimension and surface finish in turning AISI-1060 steel. J Zhejiang Univ Sci A 7(11):1790–1799
9. Sivaiah P, Chakradhar D (2017) Machinability studies on 17-4 PH stainless steel under cryogenic cooling environment. Mater Manuf Process 32(15):1775–1788
10. Potta Sivaiah (2019) Effect of cryogenic coolant on turning performance: a comparative study. SN Appl Sci 1(1):67
11. Sivaiah P, Chakradhar D (2018) Effect of cryogenic coolant on turning performance characteristics during machining of 17-4 PH stainless steel: a comparison with MQL, wet, dry machining. CIRP J Manuf Sci Technol 21:86–96
12. Montgomery DC (2001) Design and analysis of experiments, vol 52, 5th edn. Wiley, pp 218–286
13. Thiele JD, Melkote SN (1999) Effect of cutting edge geometry and workpiece hardness on surface generation in the finish hard turning of AISI 52100 steel. J Mater Process Technol 94(2–3):216–226
14. Arbizu IP, Perez CL (2003) Surface roughness prediction by factorial design of experiments in turning processes. J Mater Process Technol 143:390–396
15. Choudhury IA, El-Baradie MA (1997) Surface roughness prediction in the turning of high-strength steel by factorial design of experiments. J Mater Process Technol 67(1–3):55–61
16. Sarikaya M, Gullu A (2014) Taguchi design and response surface methodology based analysis of machining parameters in CNC turning under MQL. J Clean Prod 65:604–616
17. Sarıkaya M, Yılmaz V, Güllü A (2016) Analysis of cutting parameters and cooling/lubrication methods for sustainable machining in turning of Haynes 25 superalloy. J Clean Prod 133:172–181
18. Gupta MK, Sood PK, Sharma VS (2016) Machining parameters optimization of titanium alloy using response surface methodology and particle swarm optimization under minimum quantity lubrication environment. Mater Manuf Process 31(13):1671–1682
19. Palanisamy D, Senthil P (2016) Machinability study of laser surface treated 15-5 PH stainless steel. Mater Manuf Process 31(13):1755–1762
20. Yıldırım ÇV, Kıvak T, Sarıkaya M, Erzincanlı F (2017) Determination of MQL parameters contributing to sustainable machining in the milling of nickel-base superalloy waspaloy. Arab J Sci Eng 42(11):4667–4681
21. Gupta MK, Mia M, Singh G, Pimenov DY, Sarikaya M, Sharma VS (2019) Hybrid cooling–lubrication strategies to improve surface topography and tool wear in sustainable turning of Al 7075-T6 alloy. Int J Adv Manuf Technol 101(1–4):55–69
22. Sarıkaya M, Güllü A (2015) Multi-response optimization of minimum quantity lubrication parameters using Taguchi-based grey relational analysis in turning of difficult-to-cut alloy Haynes 25. J Clean Prod 91:347–357
23. Sivaiah P, Chakradhar D (2018) Analysis and modeling of cryogenic turning operation using response surface methodology. Silicon 10(6):2751–2768
24. Sivaiah P, Chakradhar D (2018) Comparative evaluations of machining performance during turning of 17-4 PH stainless steel under cryogenic and wet machining conditions. Mach Sci Technol 22(1):147–162
25. Sivaiah P, Chakradhar D (2019) The effectiveness of a novel cryogenic cooling approach on turning performance characteristics during machining of 17-4 PH stainless steel material. Silicon 11(1):25–38
26. Sivaiah P, Chakradhar D (2017) Multi-objective optimisation of cryogenic turning process using Taguchi-based grey relational analysis. Int J Mach Mach Mater 19(4):297–312
27. Sivaiah P, Chakradhar D (2018) Multi performance characteristics optimization in cryogenic turning of 17-4 PH stainless steel using Taguchi coupled grey relational analysis turning of 17-4 PH stainless steel using Taguchi coupled grey. Adv Mater Process Technol 4(3):431–447
28. Sivaiah P, Chakradhar D (2019) Performance improvement of cryogenic turning process during machining of 17-4 PH stainless steel using multi objective optimization techniques. Measurement 136:326–336
29. Sivaiah P, Chakradhar D (2019) Modeling and optimization of sustainable manufacturing process in machining of 17-4 PH stainless steel. Measurement 134:142–152
30. Sivaiah P, Mallikarjuna P, Uma B, Chalapathi KV (2018) Optimization of environmental friendly turning process using Taguchi integrated grey relational analysis during machining of 17-4 PH stainless steel. i-Manager's J Mech Eng 8(4):8–16
31. Sampaio MA, Machado AR, Laurindo CAH, Torres RD, Amorim FL (2018) Influence of minimum quantity of lubrication (MQL) when turning hardened SAE 1045 steel: a comparison with dry machining. Int J Adv Manuf Technol 98(1–4):959–968
32. Tamang SK, Chandrasekaran M, Sahoo AK (2018) Sustainable machining: an experimental investigation and optimization of machining Inconel 825 with dry and MQL approach. J Braz Soc Mech Sci Eng 40(8):374
33. Stephan DD, Werner J, Yeater RP (1998) Essential regression and experimental design for chemists and engineers. MS Excel Add Software Package, vol 2001
34. Seeman M, Ganesan G, Karthikeyan R, Velayudha A (2010) Study on tool wear and surface roughness in machining of particulate aluminum metal matrix composite-response surface methodology approach. Int J Adv Manuf Technol 48(5–8):613–624
35. Aouici H, Yallese MA, Fnides B, Chaoui K, Mabrouki T (2011) Modeling and optimization of hard turning of $X_38CrMoV_{5\text{-}1}$ steel with CBN tool: machining parameters effects on flank wear and surface roughness. J Mech Sci Technol 25(11):2843–2851